EPJ Web of Conferences **95**, 04062 (2015)
DOI: 10.1051/epjconf/ 20159504062

LHC signals of the SO(5)×U(1) gauge-Higgs unification

Takuya Shimotani[1,a]

[1] *Department of Physics, Osaka University, 1-1 Toyonaka, Osaka 560-0043, Japan*

Abstract. We study the LHC signals of SO(5)×U(1) gauge-Higgs unification as a beyond the standard model (SM). When the extra dimensional space is not simply-connected, dynamics of the Aharonov-Bohm (AB) phase, θ_H, in the extra dimension can induce dynamical gauge symmetry breaking by the Hosotani mechanism. The Kaluza-Klein (KK) mass spectra of γ, Z, Z_R and Higgs self couplings obey universal relations with θ_H in the fifth dimension. In our model, three neutral gauge bosons, Z' bosons, appear at TeV scale. Z' bosons are the first KK modes $Z_R^{(1)}$, $Z^{(1)}$, and $\gamma^{(1)}$. We analyze Z' bosons through dilepton events at LHC. For $\theta_H = 0.114$, the mass and decay width of $Z_R^{(1)}$, $Z^{(1)}$, and $\gamma^{(1)}$ are (5.73, 482), (6.07, 342), and (6.08 TeV, 886 GeV), respectively. For $\theta_H = 0.073$ their masses are $8.00 \sim 8.61$ TeV. An excess of events in the dilepton invariant mass should be observed in the Z' search at the upgraded LHC at 14 TeV.

1 Introduction

A Higgs boson has been discovered by LHC experiments. This discovery supports the standard model(SM) as a unified theory of electroweak symmetry. However, the SM does not contain the dark matter and the SM has Higgs quadratic divergence problem. To solve these problems we introduce gauge-Higgs unification(GHU) as a beyond the SM.

The GHU is formulated in higher dimensional gauge theory. The four-dimensional Higgs boson appears as a part of components of gauge fields. When the extra dimension is non-simply connected space, for example a circle, we introduce Wilson loop which integrates gauge fields along extra dimensions. This Wilson loop can have a constant phase θ_H, like the Aharonov-Bohm(AB) phase,

$$e^{i\theta_H} = P \exp\left\{ ig \int_0^{2\pi R} dy \, \langle A_y \rangle \right\}, \tag{1}$$

where A_y is the extra dimensional component of gauge fields and θ_H is AB phase. This AB phase breaks the gauge symmetry. This mechanism is called Hosotani mechanism[1, 2]. Then we introduce a Higgs field as a fluctuation of this AB phase. In gauge-Higgs unification electroweak symmetry is broken by this phase[3]. This phase cannot be removed because Wilson loop is gauge invariant. If one wants to remove this AB phase by gauge transformation, this phase appears the boundary condition again. In this scenario we do not consider Higgs quadratic divergence because 1-loop effective potential and Higgs mass are finite by using this mechanism. This phase is dynamically determined by a minimum of 1-loop effective potential. Because we do not introduce a scalar field,

[a] e-mail: shimon@het.phys.sci.osaka-u.ac.jp

GHU is strongly restricted by gauge principle. Although this mechanism have interesting feature, this is not proved all order calculation. Recent year SU(3) model is calculated by lattice gauge theory as a non-pertarbative method[4].

Now we introduce the SO(5)×U(1) GHU as a realistic model[5–7]. At low energies this model yields almost the same results as the SM[7]. To distinguish the GHU from the SM we examine the prediction of new particles. Our model has Z's which are not the SM Z boson but neutral massive gauge bosons. In this paper we discuss Z' search of our model at LHC experiments[10].

2 The SO(5)×U(1) gauge-Higgs unification

In this section we define the SO(5)×U(1) GHU. We introduce $SU(3)_C \times SO(5) \times U(1)_X$ gauge field on the Randall-Sundrum warped space-time. A Higgs doublet is introduced in the coset part SO(5)/SO(4). The standard model fermions are vector representation on the bulk region. We need brane fermions to construct the mass difference of top and bottom quarks. $SO(5) \times U(1)_X$ symmetry is broken to $SO(4) \times U(1)_X$ symmetry by boundary condition of the extra dimension. SO(4) symmetry is equivalent to $SU(2)_L \times SU(2)_R$ symmetry. In this case, this model has custodial symmetry. The Peskin-Takeuchi T parameter should be zero[9]. $SU(2)_R \times U(1)_X$ symmetry is broken by the brane scalar which is introduced at a brane. In this time, these gauge bosons are massive, we call W_R and Z_R. Z_R is neutral. $SU(2)_L \times U(1)_Y$ symmetry is broken by Hosotani mechanism. The first KK gauge bosons $Z_R^{(1)}, Z^{(1)}, \gamma^{(1)}$ are the candidates of Z' bosons because we do not have Kaluza-Klein(KK) parity. $H \to \gamma\gamma$ process leads us to $\theta_H \sim 0.2$. In this region we predict Z' mass are more than 3 TeV, Table 1.

At this time 1-loop effective potential has minimum at $\theta_H = \pi/2$ because all fields are same periodicity. Our Higgs couplings are proportional to $\cos\theta_H$. In the case of $\theta_H = \pi/2$, Higgs coupling is zero. Higgs boson becomes stable and cannot be observed. To avoid this we introduce dark fermions. This fermions are another periodicity because this fermion is spinorial representation. Therefore we can move a minimum of effective potential.

Then this model has seven parameters $g_A, g_B, k, z_L, c_t, c_F, n_F$. Adjusting theses parameters, we reproduce the values of five observed quantities $m_Z, g_w, \sin^2\theta_W, m_t, m_H$. Especially, dark fermion mass is fixed by Higgs mass $m_H = 126$ GeV. Parameters and masses in the case of degenerate dark fermions with $n_F = 5$ is Table 1. We can change warp factor, the number of dark fermions and $U(1)_X$ charge Q_X. When warp factor is small, KK mass is heavy. If we choose large Q_X, $H \to \gamma\gamma$ process is enhanced. And also when $Q_X = 1/2$ we can get the neutral dark fermions. If we assume conservation of the number of dark fermions, the dark fermions can become stable. In this scenario dark fermions are one of dark matter candidates[8].

Table 1. Parameters and masses in the case of degenerate dark fermions with $n_F = 5$. All masses and k are given in units of TeV.

z_L	θ_H	m_{KK}	k	c_t	c_F	$m_{F^{(1)}}$	$m_{Z_R^{(1)}}$	$m_{Z^{(1)}}$	$m_{\gamma^{(1)}}$
10^9	0.473	2.50	7.97×10^8	0.376	0.459	0.353	1.92	1.97	1.98
10^8	0.351	3.13	9.97×10^7	0.357	0.445	0.502	2.40	2.48	2.48
10^7	0.251	4.06	1.29×10^7	0.330	0.430	0.735	3.11	3.24	3.24
10^6	0.172	5.45	1.74×10^6	0.292	0.410	1.11	4.17	4.37	4.38
10^5	0.114	7.49	2.38×10^5	0.227	0.382	1.75	5.73	6.07	6.08
10^4	0.0730	10.5	3.33×10^4	0.0366	0.333	2.91	8.00	8.61	8.61

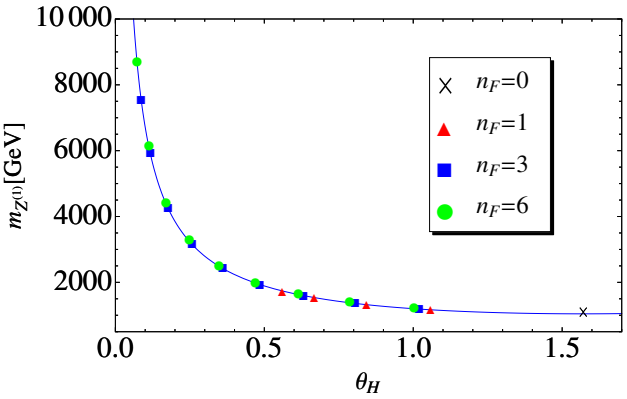

Figure 1. θ_H vs $m_{Z^{(1)}}$ for $m_H = 126\,\text{GeV}$ with n_F degenerate dark fermions.

3 The universality

In previous section we introduce dark fermions. Thess fermions need to construct observable Higgs boson. However we found the quantities which are independent on dark fermions. We call universality. See Figure 1. Colors of dots are the number of dark fermions. As you can see, all dots on the same line. This means 1st KK Z boson mass is independent on the existence of dark fermions. We also found this universal relation of masses of m_{KK}, $Z_R^{(1)}$ and $\gamma^{(1)}$. Interpolated lines of these masses are described,

$$m_{\text{KK}} \sim \frac{1352\text{GeV}}{(\sin\theta_H)^{0.786}}, \quad m_{Z_R^{(1)}} \sim \frac{1038\text{GeV}}{(\sin\theta_H)^{0.784}},$$
$$m_{Z^{(1)}} \sim \frac{1044\text{GeV}}{(\sin\theta_H)^{0.808}}, \quad m_{\gamma^{(1)}} \sim \frac{1056\text{GeV}}{(\sin\theta_H)^{0.804}}. \tag{2}$$

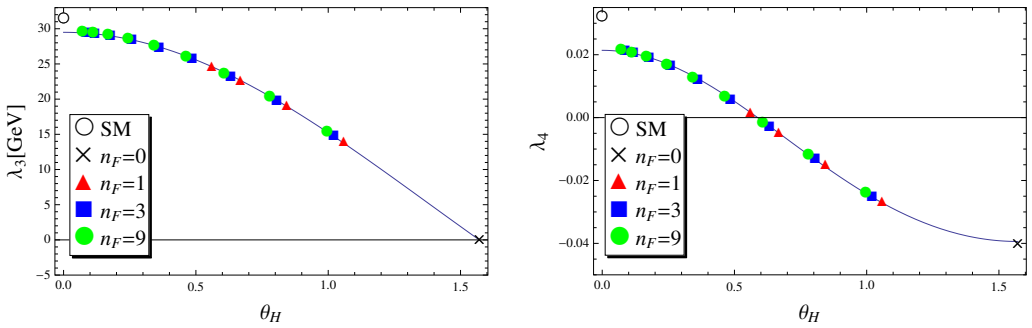

Figure 2. θ_H vs λ_3^H and λ_4^H for $m_H = 126\,\text{GeV}$ with n_F degenerate dark fermions. In the SM $\lambda_3^{\text{SM}} = 31.5\,\text{GeV}$ and $\lambda_4^{\text{SM}} = 0.0320$. The fitting curves are given by eq.(3).

In Figure 2 show the Higgs triple coupling and quartic coupling. These numbers should be compared with $\lambda_3^{\text{SM}} = 31.5$ GeV and $\lambda_4^{\text{SM}} = 0.0320$ in the SM. Interpolated lines of these couplings are

described,

$$\lambda_3/\mathrm{GeV} \sim 26.7\cos\theta_H + 1.42(1+\cos 2\theta_H),$$
$$\lambda_4 \sim -0.0106 + 0.0304\cos 2\theta_H + 0.00159\cos 4\theta_H. \quad (3)$$

This universal relation is a strong tool for predictions. Once you know the θ_H, you can know the other parameters by using the this relation. And we can ignore dark fermions unless dark fermion is the leading contribution. As a result, our free parameter is only warp factor.

Higgs mass depends on KK mass and dark fermions. Once KK mass and dark fermions are given, θ_H is determined dynamically. When we ignore dark fermion, Higgs mass has only KK mass dependence which depends on warp factor. Since the Higgs mass is given, Higgs mass has no degree of freedom. Change of warp factor is absorbed as change of θ_H.

4 Z' search

Experiments[11][12][13] show us no Z' up to 3 TeV. We analyze Z' search of 8 TeV and 14 TeV LHC [10]. In previous section we comment that Z' is independent on dark fermions because of universality. Therefore, we ignore the existence of dark fermions. We use Wilson line phase as a free parameter.

We investigate $p\bar{p} \to l^+l^-Z'$ process at tree level. Table 2 shows numerical result of couplings of $Z'q\bar{q}$ and $Z'l\bar{l}$ with $\theta_H = 0.114$. L and R of subscripts mean chirality. Z's are strongly coupled with the right-handed fermions compared with Z boson. This couplings lead to larger width of Z' than width of the SM Z boson.

Table 2. Masses, total decay widths and couplings of the Z' bosons to SM particles in the first generation for $\theta_H = 0.114$. Couplings to μ are approximately the same as those to e.

Z'	m(TeV)	Γ(GeV)	$g^{Z'}_{uL}$	$g^{Z'}_{dL}$	$g^{Z'}_{eL}$	$g^{Z'}_{uR}$	$g^{Z'}_{dR}$	$g^{Z'}_{eR}$
Z	0.0912	2.44	0.257	−0.314	−0.200	−0.115	0.0573	0.172
$Z^{(1)}_R$	5.73	482	0	0	0	0.641	−0.321	−0.978
$Z^{(1)}$	6.07	342	−0.0887	0.108	0.0690	−0.466	0.233	0.711
$\gamma^{(1)}$	6.08	886	−0.0724	0.0362	0.109	0.846	−0.423	−1.29
$Z^{(2)}$	9.14	1.29	−0.00727	0.00889	0.00565	−0.00548	0.00274	0.00856

Figure 3 shows the differential cross section multiplied by an integrated luminosity of 20.6 fb^{-1} for $pp \to \mu^+\mu^-X$ at the 8 TeV LHC for $\theta_H = 0.114$ (red solid curve) and for $\theta_H = 0.251$ (blue dashed curve). The case of $\theta_H = 0.114$ is consistent with the SM prediction. However, $\theta_H = 0.251$ case cannot explain the standard model. At invariant mass $M_{\mu\mu} = 2$ TeV, we observe the tail of the Z' resonance. The number of events is deviated 87 times as many as events of the SM prediction. Therefore, allowed region is $\theta_H < 0.251$ and $m_{Z'} > 3$ TeV.

And at 14 TeV LHC experiments, we expect the GHU signal. Figure 4 shows the differential cross section for $pp \to \mu^+\mu^-X$ at the 14 TeV LHC for $\theta_H = 0.114$ (red solid curve) and for $\theta_H = 0.073$ (blue dashed curve). The nearly straight line represents the SM background. The red line shows $\theta_H = 0.114$, $m_{Z^{(1)}_R} = 5.73$ TeV, $m_{Z^{(1)}} = 6.07$ TeV and $m_{\gamma^{(1)}} = 6.08$ TeV. Blue dashed line shows $\theta_H = 0.073$, $m_{Z^{(1)}_R} = 8.00$ TeV, $m_{Z^{(1)}} = 8.61$ TeV and $m_{\gamma^{(1)}} = 8.61$ TeV. We have two peaks of $Z^{(1)}_R$ and $Z^{(1)}, \gamma^{(1)}$ because $Z^{(1)}$ and $\gamma^{(1)}$ have almost same mass. One sees a very large deviation from the SM, which can be detected at the upgraded LHC. In $\theta_H = 0.114$ case, differential cross section at 3 TeV (4 TeV) is 13 times (86 times) as many as the SM prediction.

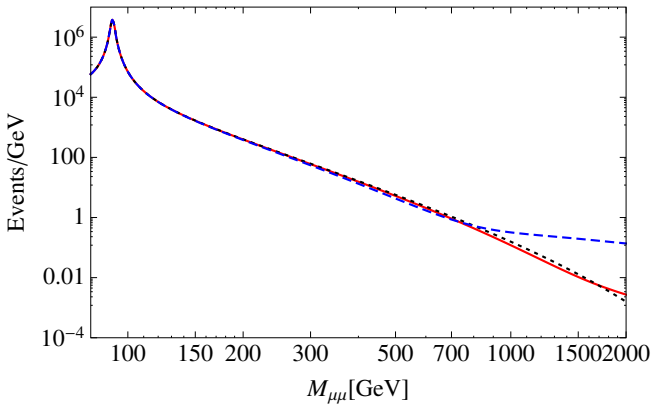

Figure 3. The differential cross section multiplied by an integrated luminosity of 20.6 fb^{-1} for $pp \to \mu^+\mu^- X$ at the 8 TeV LHC for $\theta_H = 0.114$ (red solid curve) and for $\theta_H = 0.251$ (blue dashed curve). The black dashed line represents the SM background.

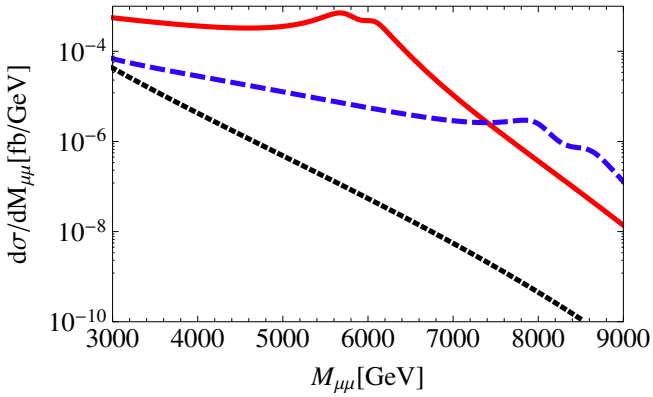

Figure 4. The differential cross section for $pp \to \mu^+\mu^- X$ at the 14 TeV LHC for $\theta_H = 0.114$ (red solid curve) and for $\theta_H = 0.073$ (blue dashed curve) . The nearly straight line represents the SM background.

5 Conclusion

In this paper, we discussed the LHC signal of SO(5)×U(1) gauge-Higgs unification. The first KK modes $Z_R^{(1)}$, $Z^{(1)}$, and $\gamma^{(1)}$, appear as Z' bosons in dilepton events at LHC. We analyzed dilepton process at 8 TeV and 14 TeV LHC experiences. Z's are strongly coupled with right-handed fermions. This leads large width of Z' (Figure 4). According to current data, we expected θ_H smaller than 0.2, Z' mass larger than 3 TeV. Figure 4 shows a large deviation from the SM. Therefore, in this case, next LHC experiments will find the Z' in the 3 TeV - 9 TeV range. If Z' bosons discover at upgraded LHC experiments, we can estimate KK mass and Higgs triple and quartic couplings by using the universal relation eq.(2)(3). This is the strong tool for the prediction. Our model is testable and outstanding model of extra dimensional theories.

References

[1] Y. Hosotani, Phys.Lett. B **126**, 309 (1983).
[2] Y. Hosotani, Annals Phys. **190**, 233 (1989).
[3] H. Hatanaka, T. Inami, and C.S. Lim, Mod. Phys. Lett. A **13**, 2601 (1998).
[4] G. Cossu, H. Hatanaka, Y. Hosotani and J. I. Noaki, Phys. Rev. D 89, 094509 (2014)
[5] Y. Hosotani, K. Oda, T. Ohnuma, and Y. Sakamura, Phys. Rev. D **78**,096002(2008); *Erratum*-ibid **79**, 079902 (2009).
[6] Y. Hosotani, S. Noda, and N. Uekusa, Prog. Theor. Phys. **123**, 757 (2010).
[7] S. Funatsu, H. Hatanaka, Y. Hosotani, Y. Orikasa, and T. Shimotani, Phys. Lett. B **722**, 94 (2013).
[8] S. Funatsu, H. Hatanaka, Y. Hosotani, Y. Orikasa and T. Shimotani, Prog. Theor. Exp. Phys. **2014**, no. 11, 113B01 (2014)
[9] M. E. Peskin and T. Takeuchi, Phys. Rev. Lett. **65**, 964 (1990).
[10] S. Funatsu, H. Hatanaka, Y. Hosotani, Y. Orikasa and T. Shimotani, Phys. Rev. D **89**, 095019 (2014).
[11] J. Alcaraz *et al.* [ALEPH and DELPHI and L3 and OPAL and LEP Electroweak Working Group Collaborations], hep-ex/0612034.
[12] [ATLAS Collaboration], ATLAS-CONF-2013-017.
[13] CMS Collaboration [CMS Collaboration], CMS-PAS-EXO-12-061.